Dynamic Properties of Firoozkooh Sand-Silt Mixtures

Ali Shafiee[1], Rouzbeh Dabiri[2], and Faradjollah Askari[3]*

1. Assistant Professor, California State Polytechnic University, Pomona
2. Assistant Professor, Department of Civil Engineering, Tabriz Branch, Islamic Azad University, Tabriz, Iran, * Corresponding Author; email: rouzbeh_dabiri@iaut.ac.ir
2. Associate Professor, Geotechnical Engineering Research Center, International Institute of Earthquake Engineering and Seismology (IIEES), Tehran, Iran

Received: 10/06/2016
Accepted: 07/11/2017

ABSTRACT

A series of undrained resonant column, monotonic and cyclic triaxial tests was performed to investigate the effects of non-plastic fines on the dynamic properties of Firoozkooh sand. Specimens of sand-silt mixtures were prepared at different densities, and tested under various confining pressures. Test results revealed that shear modulus decreases with fines, and increases with relative density and confining pressure. Normalized shear modulus is not affected by fines, relative density and confining pressure, while damping ratio is affected by fines and confining pressure. Finally, field cyclic resistance ratios versus normalized shear wave velocity values are developed on the basis of cyclic triaxial and resonant column tests.

Keywords:
Firoozkooh sand; Non-plastic silt; Shear modulus; Damping ratio; Cyclic resistance; Shear wave velocity

1. Introduction

Determination of dynamic deformation properties (i.e., shear modulus and damping ratio) of soil materials is an important step in characterization of their dynamic behavior. Although empirical relationships for the dynamic properties of sands [1-3] have been developed well, these relationships for sand-non-plastic silt mixtures, if found, are rare. It is customary to use modulus reduction and damping curves of granular soils for sand-non-plastic silt mixtures. Hence, similar to sands and gravels, normalized modulus and damping ratio should not depend on relative density, but should depend on confining pressure, in such a manner that normalized shear modulus increases and damping ratio decreases with increase in confining pressure [4-5]. Among the modulus reduction and damping curves for granular soils, the Darendeli [5] model seems to match better for sand-non-plastic silt mixtures, since it considers grain size distribution by incorporating coefficient of uniformity (C_u) in the dynamic properties model. Salgado et al. [6] investigated the maximum shear modulus (G_{max}) of sand-silt mixtures, which were prepared by the slurry deposition method, and contained up to 20% silt. They calibrated Hardin and Richart [7] and Jamiolkowski et al. [8] models to obtain two different relationships for in terms of void ratio, silt content, and initial confining pressure. On the other hand, standard materials are used as a basis to characterize fundamental mechanical behavior of soils. Toyoura, Ottawa and Fontainebleau sands are some examples of the standard materials that are widely used by the geotechnical engineers and researchers throughout the world. Unfortunately, such standard material does not exist in Iran. Recently, Iranian institutions decided to work on Firoozkooh sand as an Iranian standard material. Firoozkooh mine is situated 60 km away from

north of Tehran. The predominant formation of the region is Fajan that is composed of conglomerate and sandstone conglomerate, and belongs to the Paleocene period. The area has faced severe erosion. Recently, Ghalandarzadeh and Bahadori [9] and Bahadori et al. [10] studied the effects of stress anisotropy on the behavior of Firoozkooh sand. However, it seems that more studies are needed to quantify the mechanical behavior of Firoozkooh sand, particularly dynamic deformation properties (including shear modulus and damping ratio), which is a need for equivalent linear and non-linear analyses.

This paper aims to study the dynamic deformation properties (i.e., shear modulus and damping ratio) and liquefaction resistance of Firoozkooh sand and its mixture with non-plastic silt. It is attempted to cover the gaps in the context of dynamic behavior of sand-silt mixtures in geotechnical literature. Dynamic properties in small and large strains are evaluated on the basis of the resonant column and cyclic triaxial tests conducted on the Firoozkooh sand-silt mixtures. As a companion to the dynamic tests, monotonic triaxial tests were also carried out to explore the static liquefaction behavior of the mixtures. This paper, first, presents the static liquefaction behavior of the Firoozkooh sand-silt mixture followed by dynamic deformation properties of the mixtures, and finally, cyclic resistance versus shear wave velocity curves are developed based on the cyclic triaxial and resonant column tests.

2. Materials and Experimental Method

The study described herein investigates the effects of non-plastic silt content on the shear modulus, damping ratio and the shear wave velocity-based cyclic resistance of Firoozkooh sand using undrained cyclic triaxial and resonant column tests. The systems used for conducting tests were automated triaxial testing and fixed-free type, torsional resonant column apparatus. A detailed description of the soils used, sample preparation technique and tests procedures are given below.

2.1. Soils Tested

Firoozkooh sand (#161) is uniformly graded silica sand (*SP*) with a mean grain size, D_{50} of 0.25 mm, coefficient of uniformity, C_u of 1.75 and a specific gravity of 2.67. Its grains are sub-angular to sub-round in shape. The non-plastic silt used in the testing program was derived from the fine-grained portion of the Firoozkooh sand. Figure (1) shows the grain size distributions of the soils used in this study. The scanning electron microscope photographs of the sand and silt are also depicted in Figure (2). Clean sand with three mixtures of sand-silt was used in this study. The mixtures were obtained by mixing 15, 30, and 60% of silt by weight, respectively, with sand. The specimens were prepared to achieve after-consolidation relative densities of 15, 30, 60 and 75% depending

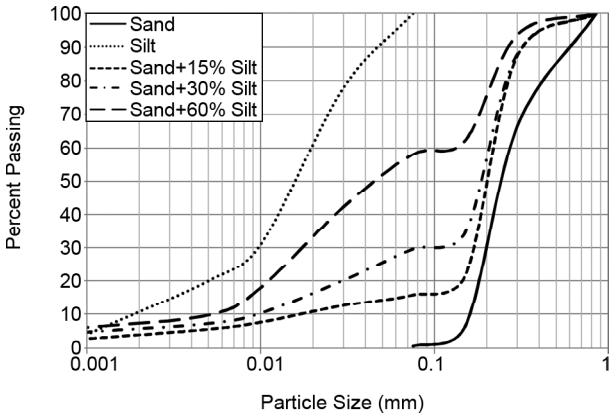

Figure 1. Grain size distribution for the soils used in this study.

(a) Sand

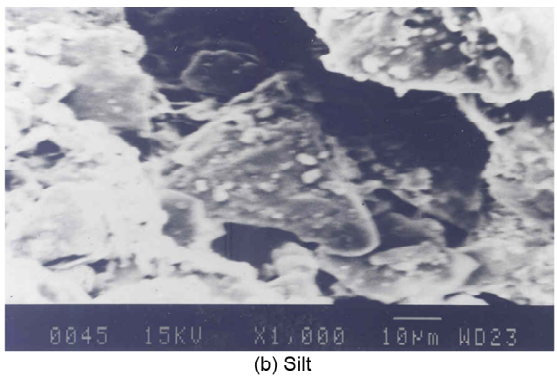

(b) Silt

Figure 2. Scanning electron microscope photograph.

Table 1. Values of void ratios for different mixtures.

Type of Materials	e_{min}	e_{max}	Dr = 15%	Dr = 30%	Dr = 60%	Dr = 75%
			e	*e*	*e*	*e*
Sand	0.58	0.87	0.83	0.78	0.69	0.65
Sand + 15% Silt	0.41	0.83	0.76	0.7	0.58	0.51
Sand + 30% Silt	0.32	0.854	0.77	0.69	0.53	0.45
Sand + 60% Silt	0.36	1.259	1.124	0.99	0.72	0.58

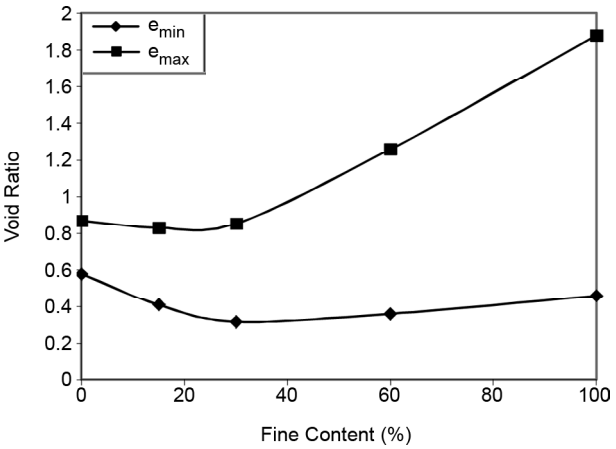

Figure 3. Variation of e_{max} and e_{min} in terms of silt content.

on their silt content. The global void ratio, e along with minimum void ratio, e_{min} and maximum void ratio, e_{max} for the mixtures are presented in Table (1). Figure (3) presents the variation of e_{max} and e_{min} in terms of silt content.

2.2. Method of Sample Preparation

In order to obtain a uniform density throughout the specimen, the undercompaction technique [11] was used. The procedure consists of placing each layer at a density slightly greater than the density of the layer below it to account for the decrease in volume and the increase in density that occurs in the lower layers when a new layer is placed on it. The specimens were made of six layers with an undercompaction value of 5%, so that the relative density varied by 1% per layer. To ensure uniform density throughout the specimen height, the void ratio distribution within the specimen was obtained by solidifying a specimen using a gelatin solution [12]. The solidified specimen was then sliced into sections and the distribution of void ratio within the test specimen was determined. The measurements revealed that the relative error in achieving the required density throughout the specimens was successfully less than 5% for each layer. In addition, the specimens were prepared in a Plexiglas mold to have better control over layer thickness. During sample preparation, it was found that forming low density specimens for high silt content (i.e., 60%) materials was impossible because of excessive collapse during the saturation. Thus, high silt content specimens were prepared at high relative densities of 60 and 75%, meanwhile other specimens were prepared at densities of 15, 30 and 60%.

2.3. Test Setup

Resonant column and cyclic and monotonic triaxial tests were run in this study. Small-strain shear wave velocity and strain dependent-shear modulus (G) of sand-silt mixtures were obtained by a fixed-free type torsional resonant column apparatus in small shear strain amplitude (i.e. $10^{-6}<\gamma<10^{-4}$). The tested specimens were typically 70 mm in diameter and 100 mm in height. The specimens were saturated with a Skempton B-value in excess of 98%, under application of a 100 kPa back pressure. To facilitate the saturation process, carbon dioxide (CO_2) was first percolated through the specimens. Following the saturation, specimens were isotropically consolidated under three effective confining pressures of 100, 200 and 300 kPa. All the relative densities reported herein are based on the after-consolidation void ratios.

All the monotonic and cyclic triaxial tests were run on the specimens with a typical diameter of 70 mm and a height of 150 mm. The sample preparation technique and saturation procedure were similar to the ones in resonant column tests. In the cyclic triaxial tests, the specimens were loaded sinusoidally at a frequency of 0.1 Hz under stress-controlled condition [13] at the appropriate cyclic stress ratio until they liquefied under an initial confining pressure of 100 kPa. Monotonic triaxial test was also performed on the sand-silt mixtures under three effective confining pressures of 100, 200 and 300 kPa.

3. Test Results and Discussion

3.1. Static Liquefaction of the Firoozkooh Sand-Silt Mixtures

To explore all features of liquefaction behavior of Firoozkooh sand, 33 undrained monotonic triaxial tests were conducted on sand-silt mixtures. The effective stress paths on the $p'-q$ diagram ($p'=$ mean effective confining stress, and q = deviatoric stress) for all the tested materials are shown in Figure (4). The steady state line, SSL [14] is typically shown for the clean sand prepared at a relative density of 60% (Figure 4a). It is observed that in the clean sand and sand-silt mixtures containing up to 30% silt flow liquefaction occur, as was previously shown by Yamamuro and Lade [15], and Lade and Yamammuro [16]. However, the mixtures with 60% silt content exhibit flow liquefaction with limited deformation [17] (Figure 4d). Table (2) shows steady state angle of friction (φ'_{SS}). As seen, φ'_{SS} decreases with fines content.

3.2. Shear Modulus and Damping Ratio of Firoozkooh Sand-Silt Mixtures

Shear modulus and damping ratio are important input parameters in dynamic analyses. To explore all features of the dynamic behavior of Firoozkooh sand, it was decided to evaluate the dynamic deformation properties of the Firoozkooh sand-silt mixtures. Figure (5) show the effects of non-plastic fines on the shear modulus of Firoozkooh sand at different relative densities and confining pressures. The experimental results clearly show that at an identical relative density and effective confining pressure, shear modulus decreases when fines content is raised. As shown, shear modulus of clean sand is reduced up to 40% when silt content is 60%. Hence, a weaker structure would be formed when fines content is raised. It can also be inferred that in all the mixtures, shear modulus increases with relative density and confining pressure. Next, on the basis of the shear modulus obtained at very low shear

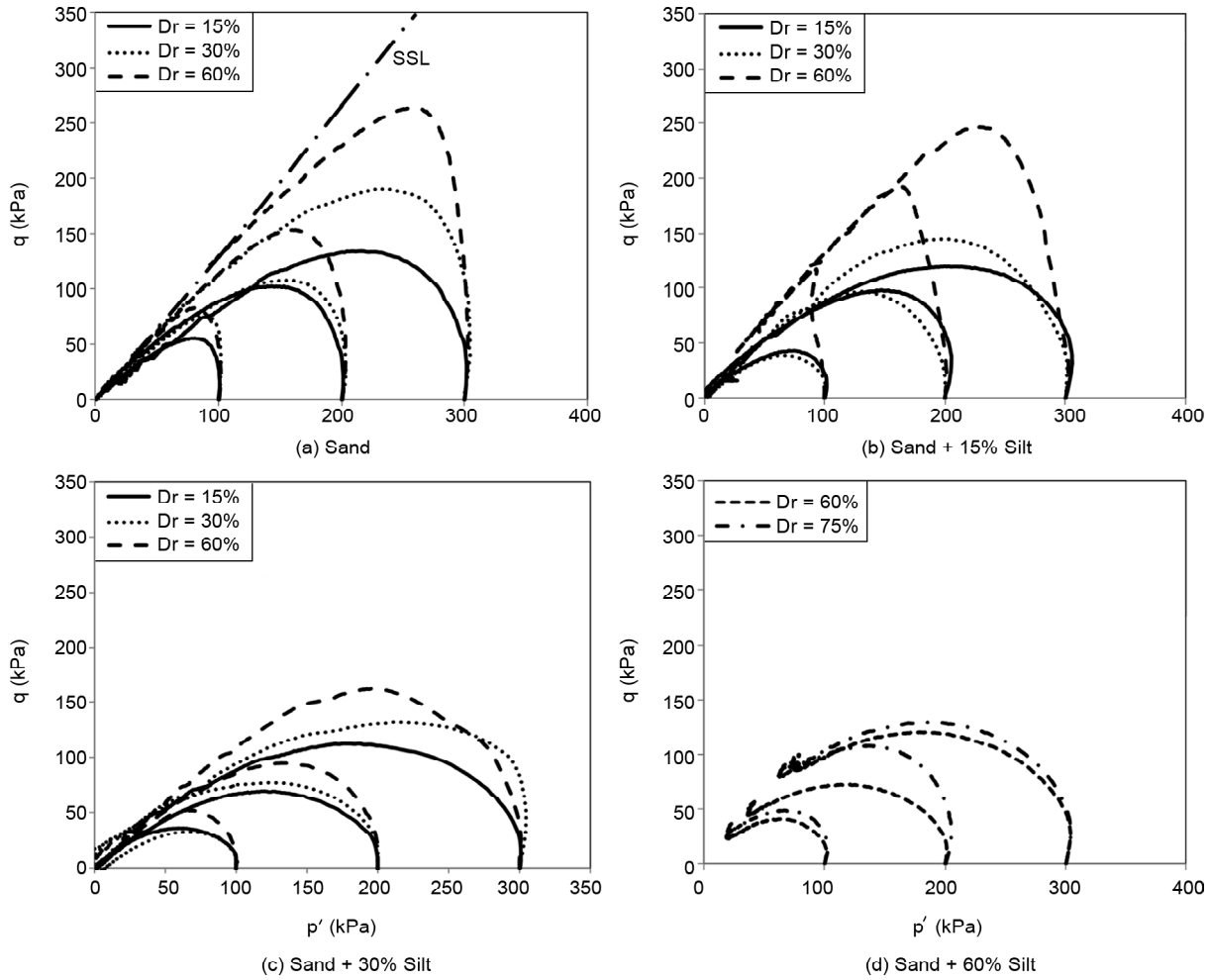

Figure 4. Effective stress path for Firoozkooh sand-silt mixtures under monotonic triaxial loading.

strains (i.e. $\gamma \approx 10^{-6}$), a mathematical model for maximum shear modulus of Firoozkooh sand-silt mixtures was developed. Form of the model was based on the Hardin and Richart [7] equation that states the maximum shear modulus in sands can be presented as:

$$G_{\max} = AF(e)(p_0')^n \quad (1)$$

in which A is an empirical constant reflecting soil fabric formed through various stress and strain histories, n is empirically determined exponent, approximately equal to 0.5 [18], $F(e)$ is a void ratio function, and p_0' is initial mean confining pressure.

It was shown (Figure 5) that shear modulus is a function of silt content, confining pressure and relative density or void ratio. Hence, to characterize the low-amplitude dynamic properties of Firoozkooh sand-silt mixtures, it is necessary to find an appropriate mathematical model in the form of Equation (1). Herein, a regression analysis based on the least square technique is used to find the values

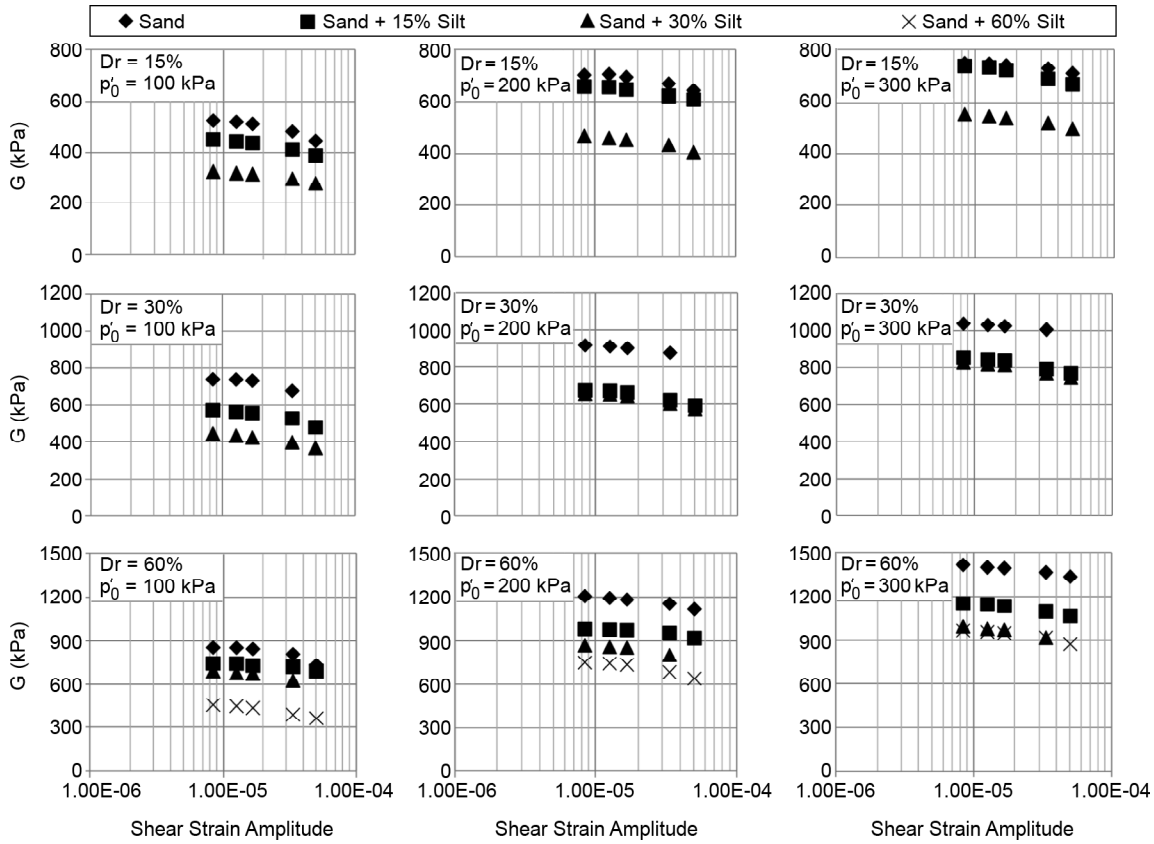

Figure 5. Effect of fines on the shear modulus of Firoozkooh sand.

Table 2. Summary of resonant column and cyclic triaxial tests results for the tested materials.

Material	Dr(%)	$\varphi'_{SS}(^\circ)$	$CRR_{triaxial}$	Vs (m/s)	α_{mean}	β	CRR_{field} (Eq.6)	CRR_{field} (Eq.9)	Vs_1 (m/s)
Clean Sand	15	20	0.096	182	0.788	1.15	0.087	0.07	170.6
	30	29	0.132	193	0.68	1.15	0.103	0.094	174.8
	60	34	0.25	201	0.63	1.3	0.201	0.15	178
Sand + 15% Silt	15	17	0.112	169	0.83	1.15	0.106	0.082	160
	30	23	0.142	181	0.752	1.15	0.123	0.1	167
	60	32	0.23	202	0.65	1.3	0.194	0.138	181
Sand + 30% Silt	15	16.2	0.061	157	0.832	1.15	0.058	0.045	149
	30	19	0.096	168	0.796	1.15	0.088	0.068	157
	60	29	0.23	189	0.68	1.3	0.203	0.138	171
Sand + 60% Silt	60	28	0.033	164	0.69	1.3	0.03	0.02	149
	75	31	0.093	175	0.66	1.45	0.088	0.048	157

of constants A and n in Equation. (1). It is supposed that $F(e)$ takes the same form as stated by Hardin and Richart [7]:

$$F(e) = (2.973 - e)^2 / (1 + e) \quad (2)$$

Then, the appropriate model for each mixture was obtained as follows:

Clean Sand:

$$G_{max} = 4528F(e)(p_0')^{0.38} \quad R^2 = 0.80 \quad (3)$$

Sand + 15% Silt:

$$G_{max} = 2977F(e)(p_0')^{0.40} \quad R^2 = 0.89 \quad (4)$$

Sand + 30% Silt:

$$G_{max} = 2116F(e)(p_0')^{0.43} \quad R^2 = 0.86 \quad (5)$$

Sand+60% Silt:

$$G_{max} = 994F(e)(p_0')^{0.59} \quad R^2 = 0.86 \quad (6)$$

where R^2 is the coefficient of determination.

Figure (6), clearly shows that A and n depend on the fines content (FC). Therefore, a general equation for Firoozkooh sand-silt mixtures can be represented as:

$$G_{max} = [-57(FC) + 4159]F(e)p_0'^{0.004(FC)+0.36} \quad (7)$$

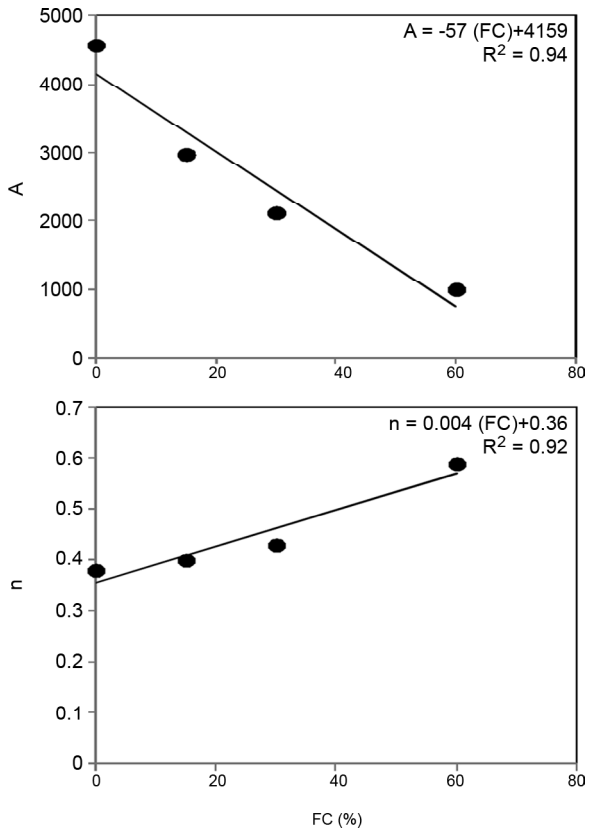

Figure 6. Variations of A and n with fines content (FC).

where FC is in percent, and G_{max} and p_0' are in kPa.

Having obtained the values of maximum shear modulus, normalized shear modulus (G/G_{max}) curves can be drawn for Firoozkooh sand-silt mixtures. Figure (7) shows the effects of fines on the normalized shear modulus of Firoozkooh sand for the range of shear strains covered by resonant column tests in this study. To have better understanding on the dynamic deformation properties of the sand-silt mixtures, normalized shear modulus curves of Seed et al. [2] have been superimposed on Figure (7). As seen, normalized shear modulus of sand-silt mixtures is independent of fines content, and fall in the upper bound region of Seed et al. [2] curves. It is also evident that G/G_{max} of clean sands and sand-silt mixtures is almost independent of relative density and confining pressure.

Figure (8) shows the effect of fines on the damping ratio of Firoozkooh sand for the range of shear strains covered by resonant column tests in this study. Curves of Seed et al. [2] have also been superimposed on Figure (8). As seen, damping ratio decreases with silt content up to 30% fines, further increase in fines content would increase damping ratio. However, damping ratio of clean sands is still more than that of the mixtures containing 60% fines. As shown, damping ratio of clean sand is reduced up to 35% when silt content is 30%. In addition, the values of damping ratio for

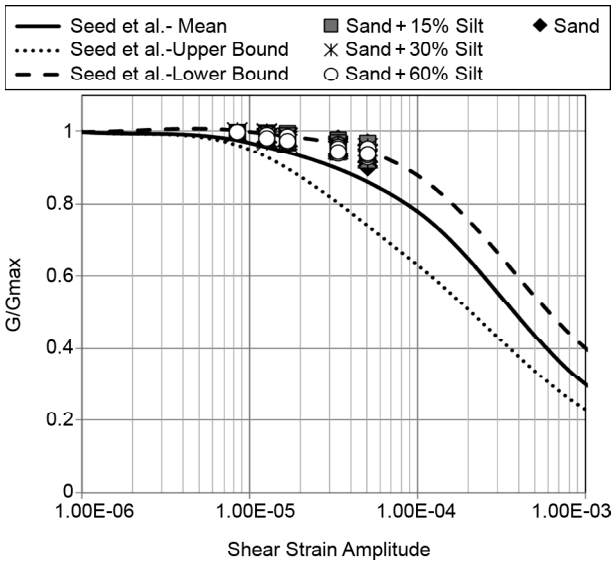

Figure 7. Effect of fines content on the normalized shear modulus of Firoozkooh sand.

Firoozkooh sand-silt mixtures fall in the lower bound region of Seed et al. [2] curves.

Figures (9) and (10) typically show the effects of relative density and confining pressure on the damping ratio of clean sands and sand-silt mixtures respectively. As seen, damping ratios of clean sands and sand-silt mixtures are almost independent of relative density, but depend somewhat on the confining pressure. As seen, the damping ratio of all the mixtures decrease with confining pressures.

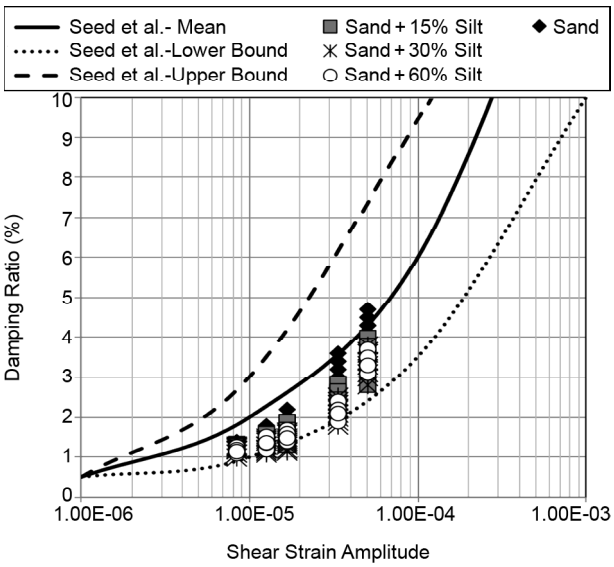

Figure 8. Effect of fines content on the damping ratio of Firoozkooh sand.

3.3 Shear Wave Velocity-Based Cyclic Resistance of Firoozkooh Sand-Silt Mixtures

Several liquefaction evaluating procedures have evolved over the past three decades since a simplified method was pioneered by Seed and Idriss [19]. The use of shear wave velocity (V_s) as an index of liquefaction resistance has a sound basis because both V_s and liquefaction resistance are similarly, but not proportionally, influenced by many of the same factors (void ratio, state stress, stress history, geologic age). The advantages of a V_s-based method have been discussed by many researchers (e.g., [20-21]). The prevailing approach involves in-situ V_s measurements at sites experiencing earthquakes, following the framework of the Seed and Idriss [19] simplified procedure and correlating the overburdened stress-corrected shear wave velocity (V_{s1}) to the magnitude-scaled

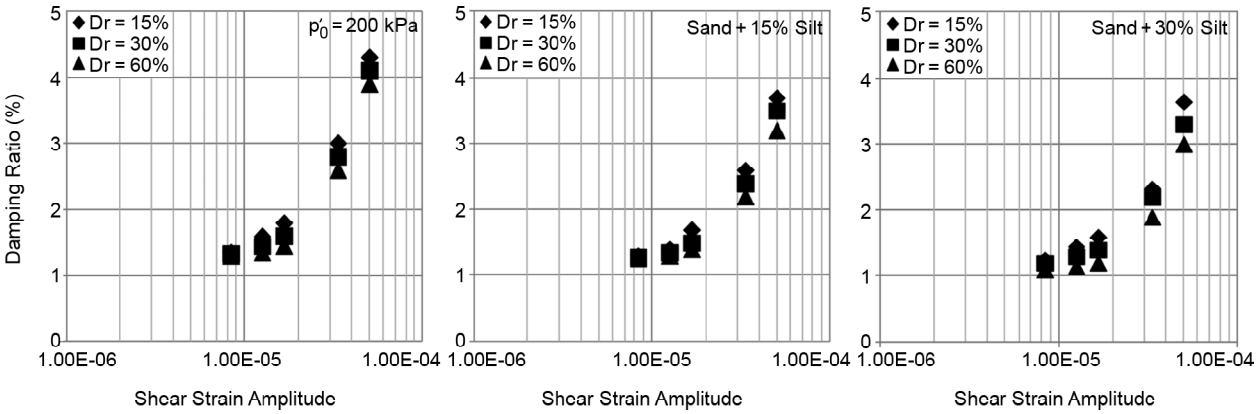

Figure 9. Effect of relative density on the damping ratio of Firoozkooh sand-silt mixtures.

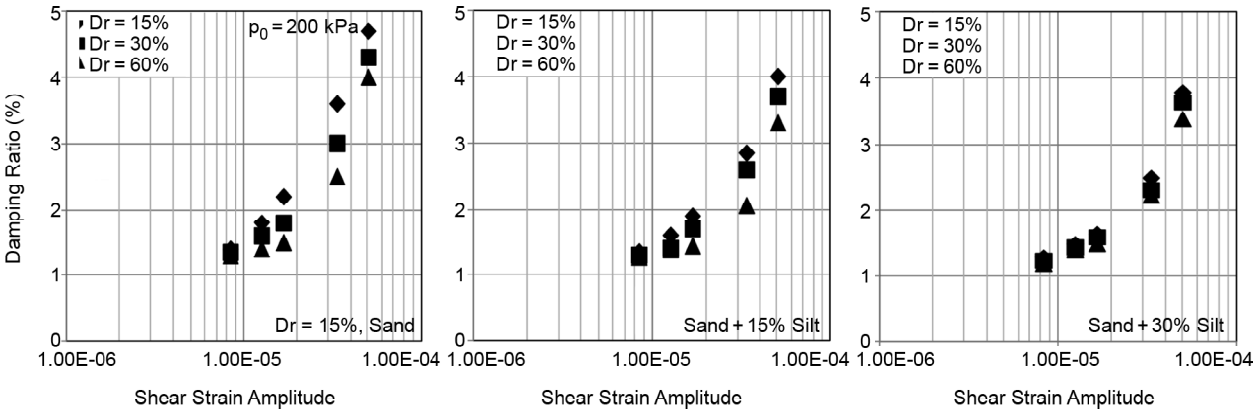

Figure 10. Effect of confining pressure on the damping ratio of Firoozkooh sand-silt mixture.

cyclic stress ratio (CSR) induced by earthquakes. However, these in-situ Vs-based methods are still less well-defined mainly because of the lack of field performance data [22]. Most measured soil parameters for in-situ V_s testing are for post-earthquake properties and do not exactly reflect the initial soil states before earthquakes. Thus, despite their great practical importance, field correlations do not furnish insight into the fundamental behavior of liquefiable soils. As pointed out by Seed and Idriss [19], if field seismic conditions are properly simulated, controlled laboratory studies can be used to broaden the applicability of liquefaction criteria, especially where little or no field performance data is available. A number of studies have focused on this subject on clean sands and sand-silt mixtures (e.g., [21, 23-27]), which demonstrated the validity of laboratory V_s-based methods.

In the present study, initial liquefaction was defined when the pore pressure in the specimen first equaled the initial confining pressure or the specimen reached 5% double amplitude axial strain, whichever occurred first. Cyclic resistance ratio ($CRR_{triaxial}$) was also calculated as the cyclic stress ratio required causing initial liquefaction in 15 cycles of loading [17]. V_s was also inferred from the $G_{\max}$ obtained from the resonant column tests as:

$$V_s = \sqrt{\frac{G_{\max}}{\rho}} \tag{8}$$

where ρ is mass density of the tested soil.

The results of cyclic triaxial and resonant column tests for this study are presented in Table (2). Both the $CRR_{triaxial}$ and V_s were obtained in the undrained cyclic triaxial and resonant column tests under isotropic consolidation conditions, which are usually different from the in-situ conditions. Therefore, some consideration should be given in applying the laboratory test-based $CRR_{triaxial}$ - V_s correlation to in situ conditions. It is common to correct CRR to in situ CRR (CRR_{field}) approximately as follows [28]:

$$CRR_{field} = \alpha.\,\beta.\,CRR_{triaxial} \tag{9}$$

where α and β are correction factors. Constant α can be presented by many equations, as follows:

$$\alpha = K_0 \tag{10}$$

$$\alpha = \frac{1+2K_0}{3} \tag{11}$$

$$\alpha = \frac{1+K_0}{2} \tag{12}$$

$$\alpha = \frac{2(1+2K_0)}{3\sqrt{3}} \tag{13}$$

in which K_0 is effective earth pressure ratio at rest. Equations (7a) and (7b) were proposed by Seed and Peacock [28] and Equations (7c) and (7d) by Finn et al. [29] and Castro [30] respectively. Coefficient K_0 was also considered as equal to $(1-\sin\varphi')$ where φ' is the angle of internal friction. For each mixture at a specific relative density, φ' was determined using monotonic undrained triaxial tests conducted under initial confining pressures of 100, 200 and 300 kPa (i.e. φ'_{SS} in Table 2). Finally, by averaging over the α values from Equations (7a) to (7d), the desired value of constant α was determined (i.e. α_{mean} in Table 2).

Constant β is a function of relative density [31] and is defined as:

$$D_r \ll 45\% \Rightarrow \beta = 1.15 \tag{14}$$

$$D_r > 45\% \Rightarrow \beta = 0.01D_r + 0.7 \tag{15}$$

Recently, Jafarian et al. [32] proposed the following relationship for CRR_{field}:

$$CRR_{field} = 0.9[-0.534\xi_R^2 + 0.095\xi_R + 0.814] \times [0.777(0.2-\xi_R)^{4.47} + 0.139] \tag{16}$$

The above equation was developed for a moment magnitude (M_w) of 7.5. ξ_R is also relative state parameter $(-0.6 \ll \xi_R \ll 0)$ as suggested by Konrad [33] and Boulanger [34]:

$$\xi_R = \frac{1}{Q - Ln\left(\frac{100p_0'}{P_a}\right)} - D_r \tag{17}$$

where P_a is the atmospheric pressure, and Q an empirical constant dependent to the mineralogy and breakage of soils, and taken equal to 10 [35]. Table (2) presents the value of CRR_{field} based on two methods for different mixtures.

On the other hand, the measured V_s requires adjustment allowing for the different stress states.

As V_s was widely observed to depend equally on principal stresses in the direction of wave propagation and particle motion [36], V_s can be expressed as:

$$V_{sf} = V_s \left[\frac{(1+2K_0)}{3} \right]^{0.25} \quad (18)$$

where V_{sf} is the equivalent field value of laboratory measured V_s. According to common practice [21] the V_{sf} in Equation (9) should be further corrected in terms of the in-situ effective overburden stress (σ'_V) as follows [30]:

$$V_{s1} = V_{sf} \left(\frac{P_a}{\sigma'_V}\right)^{0.25} = V_s \left(\frac{1+2K_0}{3}\right)^{0.25} \left(\frac{P_a}{p'_0}\right)^{0.25} \quad (19)$$

where V_{s1}= overburden stress-corrected velocity; P_a = atmospheric pressure; and p'_0 = mean effective stress in the laboratory. Table (2) presents the value of V_{s1} for each mixture.

3.3.1. Comparison of Converted Laboratory Results with Field-Based Correlation

To check the validity of the results of this study, the CRR_{field}-V_{s1} correlations developed in the laboratory for this and other laboratory-based studies are compared to the field-based correlations of Andrus and Stokoe [21] for different ranges of fines content (FC), i.e.: $FC \leq 5\%$, $5\% \prec FC \prec 30\%$, and $FC \geq 30\%$, as shown in Figure (11).

As seen, the results of this study are fairly close to the Andrus and Stokoe curves. However, most of the other laboratory-based results show a significant scatter with respect to the Andrus and Stokoe curves. Figure (11a) shows that the CRR_{field}-V_{s1} correlation for the clean sand used in this study almost lies near the semi-empirical curve proposed in the simplified procedure for fines content of less than 5%. Similarly, the trends in the laboratory data on sands with 15% fines content was found to be consistent with the liquefaction boundary curves developed by Andrus and Stokoe for $FC = 20\%$ from the field performance data (Figure 11b). As shown in Figure (11c), the laboratory-based correlations from this study for $FC = 30$ and 60% plot almost below the field-based curve for $FC \geq 30\%$; hence, using the field-based correlations would overestimate the liquefaction resistance of these sand-silt mixtures.

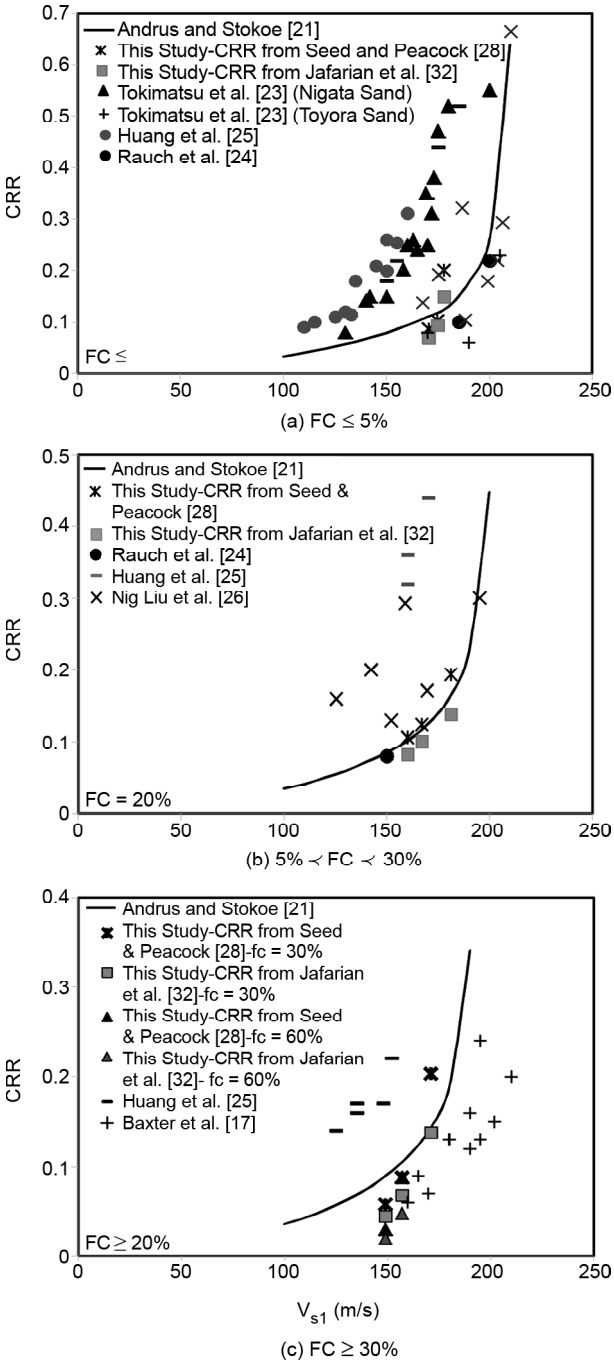

Figure 11. Comparison between converted CRRfield-Vs1 data based on the laboratory data and the existing field-based data.

As seen in Figure (11), significant differences may exist between laboratory-based correlations and the field performance data of Andrus and Stokoe [21]. This difference may originate from the inherent uncertainties in laboratory and field performance data.

4. Conclusion

An attempt has been made to evaluate dynamic behavior of Firoozkooh sand, as an Iranian standard material, and its mixtures with non-plastic fines.

Specimens were prepared at different densities and tested under different confining pressures in triaxial and resonant column apparatus. Data from previous laboratory studies on sands, silty sands and the laboratory data generated as the part of this study were also compared to field based CRR-V_{s1} curves prepared by Andrus and Stokoe [21]. The following conclusions, regarding the effects of non-plastic fines on the shear modulus and damping ratio and liquefaction susceptibility, can be drawn from this study:

- Monotonic triaxial tests revealed that the clean sand and sand-silt mixtures with silt content up to 30% exhibit flow liquefaction behavior. Meanwhile, 60% silt content mixtures show flow liquefaction with limited deformation behavior. Angle of friction in steady state also decreases with fines content;
- At an identical relative density and effective confining pressure, shear modulus decreases when fines content is raised. In addition, shear modulus increases with relative density and confining pressure;
- Maximum shear modulus of Firoozkooh sand-silt mixtures can be represented as a function of void ratio, initial confining pressure and fines content;
- Normalized shear modulus of clean sands and sand-silt mixtures is almost independent of relative density and confining pressure and the values of normalized shear modulus for the Firoozkooh sand-silt mixtures, fall in the upper bound region of Seed et al. [2] curves;
- Damping ratio decreases with silt content up to 30% fines, further increase in fines content would lead to the increase in damping ratio. Damping ratio of clean sands and sand-silt mixtures is almost independent of relative density, but depend somewhat on confining pressure, and decreases with confining pressure. In addition, the values of damping ratio for the Firoozkooh sand-silt mixtures, fall in the lower bound region of Seed et al. [2] curves.
- In conversion of laboratory data to field condition, results show that the CRR_{field}-V_{s1} correlation for the Firoozkooh clean sand and Firoozkooh sand containing up to 15% fines lie closely to the semi-empirical curve proposed in the simplified procedure by Andrus and Stokoe [21]. The CRR_{field}-V_{s1} values for FC = 30% and 60% in present research are almost below the field-based curve for , which means that field-based correlation overestimate the liquefaction resistance of these sand-silt mixtures related to the present study.

Acknowledgements

This research was conducted in and supported by the International Institute of Earthquake Engineering and Seismology (IIEES) under the Contract No.6712. This support is gratefully appreciated.

References

1. Seed, H.B. and Idriss, I.M. (1970) Soil moduli and damping factors for dynamic response analyses. *Report No. EERC 70-10, Earthquake Engineering Research Center*, Univ. of California, Berkeley, California.

2. Seed, H.B., Wong, R.T/, Idriss, I.M., and Tokimatsu, K. (1986). Moduli and damping factors for dynamic analyses of cohesionless soils. *Journal of Geotechnical Engineering*, **112**(11), 1016-1032.

3. Assimaki, D., Kausel, E., and Whittle, A. (2000) Model for dynamic shear modulus and damping for granular soils. *Journal of Geotechnical and Geoenvironmental Engineering*, **126**(10), 859-869.

4. Iwasaki, T., Tatsuoka, F., and Takagi, Y. (1978) Shear moduli of sands under cyclic torsional shear loading. *Soils and Foundations*, **18**(1), 39-50.

5. Darendeli, M.B. (2001) *Development of a New family of Normalized Modulus Reduction and Material Damping Curves*. Ph.D. Dissertation, The University of Texas, Austin.

6. Salgado, R., Bandini, P., and Karim, A. (2000) Shear strength and stiffness of silty sand. *Journal of Geotechnical and Geoenviromental Engineering*, **126**(5), 451-462.

7. Hardin, B.O. and Richart, Jr. F.E. (1963) Elastic wave velocities in granular soils. J*ournal of Soil Mechanics and Foundations Division*, ASCE, **89**(1), 33-65.

8. Jamiolkowski, M., Leroueil, S. ,and Lo Presti, D.C.F. (1991) Theme lecture: Design parameters from theory to practice. *Proceeding of Geo-Coast,* **91**, 1-41.

9. Ghalandarzadeh, A. and Bahadori, H. (2005) Effect of stress anisotropy on the cyclic behavior of saturated sand in undrained condition. *PRO of the INT. CON. on Soil Mechanics and Geotechnical Engineering*, **16**(2), 375-378.

10. Bahadori, H., Ghalandarzadeh, A., and Towhata, I. (2008) Effect of non-plastic silt on the anisotropic behavior of sand. *Journal of Soils and Foundations*, **48**(4), 30-45.

11. Ladd RS (1978) Preparing test specimens using undercompaction. *Printed by American Society for Testing and Material*, 16-23.

12. Emery, J.J/, Finn, W.D.L., and Lee, K.W. (1973) Uniformity of saturated sand samples. *ASTM Special Publishing*, 182-194.

13. ASTM D 5311 (2004) *Standard Test Method for Load Controlled Cyclic Triaxial Strength of Soil*. Annual Book of ASTM Standards, Section 4, vol. 04.08. ASTM International, West Conshohocken, PA.

14. Castro, G. (1975) Liquefaction and cyclic mobility of saturated sand. *Journal of American Society of Civil Engineering*, ASCE, **101**, 551-569.

15. Yamamuro, J.A. and Lade, P.V. (1997) Static liquefaction of very loose sands. *Canadian Geotechnical Journal*, **34**(6), 905-917.

16. Lade, P.V. and Yamamuro, J.A. (1997) Effects of nonplastic fines on static liquefaction of sands. *Canadian Geotechnical Journal*, **34**(6), 918-928.

17. Ishihara, K. (1996) *Soil Behavior in Earthquake Geotechnics*. Oxford Univ. Press, Newyork.

18. Hardin, B.O. and Drnevich, V.P. (1972) Shear modulus and damping in soils: measurement and parameter effects. *Journal of Soil Mechanics and Foundations Division*, ASCE, **98**(6), 603-624.

19. Seed, H.B. and Idriss, I.M. (1971) Simplified procedure for evaluating soil liquefaction potential. *Journal of Soil Mechanics and Foundation Division*, **97**(9), 1249-1273.

20. Youd, T.L., Idriss, I.M., Andrus, R.D., Arango, R.C., Castro, G., Christian, J.T., Dobry, R., Finn W.D.L., Harder, Jr, L.F., Hynes, M.E., Ishihara, K., Koester, J.P., Liao, S.S.C., Marcuson, I.I.I.W.F., Martin, G.R., Mitchell, J.K., Moriwaki, Y., Power, M.S., Robertson, P.K., Seed, R.B., and Stokoe, I.I.K.H. (2001) Liquefaction resistance of soils: summary report from the 1996 NCEER and 1998 NCEER/NSF workshop on evaluation of liquefaction resistance of soils. *Journal of Geotechnical and Geoenvironmental Engineering*, **127**(10), 817-833.

21. Andrus, R.D. and Stokoe, II.K.H. (2000) Liquefaction resistance of soils from shear wave velocity. *Journal of Geotechnical and Geoenvironmental Engineering*, **126**(11), 1015-1025.

22. Kayen, R., Seed, R.B., Moss, R.E., Cetin, K.O., Tanaka, Y., and Tokimatsu, K. (2004) Global shear wave velocity database for probabilistic assessment of the initiation of seismic-soil liquefaction. *11th Int. Conference on Soil Dynamics and Earthquake Engineering*, Berkeley, 7-9.

23. Tokimatsu, K., Yamazuka, T., and Yoshimi, Y. (1986) Soil liquefaction evaluations by elastic shear moduli. *Soils and Foundation*, **26**(1), 25-35.

24. Rauch, A.F., Duffy, M., and Stokoe, K. (2000) Laboratory correlation of liquefaction resistance with shear wave velocity. *Journal of Geotechnical and Geoenviromental Engineering, Geotechnical Special Publication*, **101**, 66-80.

25. Huang, Y.T., Huang, A.B., Chen, K.Y., and Dou, T.M. (2004) A laboratory study on the undrained strength of a siltysand from central western taiwan. *Journal of Soil Dynamic and Earthquake Engineering*, **24**(9-10), 733-743.

26. Ning Liu, S.M., Mitchell, J.K., and Hon, M. (2006) Influence of non plastic fines on shear wave velocity-based assessment of liquefaction.

Journal of Geotechnical and Geoenviromental Engineering, **132**(8), 1091-1097.

27. Baxter, C.D.P., Bradshaw A.S., Green R.A., and Wang, J. (2008) Correlation between cyclic resistance and shear wave velocity for providence silts. *Journal of Geotechnical and Geoenvironmental Engineering*, **134**(1), 37-46.

28. Seed, H.B. and Peacock, W.H. (1971) The Procedure for measuring soil liquefaction characteristics. *Journal of the Soil Mechanics and Foundation Division*, **97**(SM8), 1099-1119.

29. Finn, W.D.L., Pickering, D.J., and Bransby, P.L. (1971) Sand liquefaction in triaxial and simple shear tests. *Journal of the Soil Mechanics and Foundation Division*, **97**(SM4), 639-659.

30. Castro, G. (1975) Liquefaction and cyclic mobility of saturated sand. *Journal of American Society of Civil Engineering*, ASCE, **101**, 551-569.

31. Das, B.M. (1992) *Principles of Soil Dynamics*. Printed by: Pws-Kent Publishing Company.

32. Jafarian, Y., Sadeghi Abdollahi, A., Vakili, R., and Baziar, M.H. (2010) Probabilistic correlation between laboratory and field liquefaction potentials using relative state parameter index (ξ_R). *Soil Dynamic and Earthquake Engineering*, **30**, 1061-1072.

33. Konrad, J.M. (1988) Interpretation of flat plate dilatometer tests in sands in terms of the state parameter. *Geotechnique*, **38**(2), 263-277.

34. Boulanger, R.W. (2003) High overburden stress effects in liquefaction analyses. *Journal of Geotechnical and Geoenvironmental Engineering*, **129**(12), 1071-1082.

35. Bolton, M.D. (1986) The strength and dilatancy of sands. *Geotechnique*, **36**(1), 65-78.

36. Belloti, R., Jamiolkowski, J., LoPresti, D.C.F., and O'Niell, D.A. (1996) Anisotropy of small strain stiffness in Ticino sand. *Geotechnique*, **46**(1), 115-131.